PROCEEDINGS, 48th Workshop on Geothermal Reservoir Engineering
Stanford University, Stanford, California, February 6-8, 2023
SGP-TR-224

Modeling Thermal Fracturing During Operation of Enhanced Geothermal Systems: Improved Heat-Transfer Area and Reservoir Sustainability

Quanlin ZHOU

Energy Geosciences Division, Lawrence Berkeley National Laboratory, Berkeley, CA, USA

qzhou@lbl.gov

Bin CHEN

College of Water Conservancy and Hydropower Engineering, Hohai University, Nanjing, Jiangsu, China

binchen@hhu.edu.cn

Keywords: Thermal fracture, dimensionless solution, displacement discontinuity method, stability analysis, dynamic fracture spacing, geothermal reservoir.

ABSTRACT

In the current concept of an enhanced geothermal system (EGS), a pair of horizontal wells are used to circulate fluid through stimulated hydraulic fractures; reservoir sustainability and improvement during operation are critical for long-term power generation. Injecting cold fluid into a geothermal reservoir will cause significant cooling and thermal stress, possibly resulting in secondary thermal fractures perpendicular to primary hydraulic fractures and forming a well-connected fracture network for heat transfer. First, we derived analytical solutions of dimensionless fracture length $\mathcal{L}$, aperture profile $\boldsymbol{\Omega}$, and spacing $\mathcal{D}$(as well as pattern) as functions of time τ and dimensionless effective confining stress $\mathcal{T}$ using a plane strain model and the displacement discontinuity method (Chen & Zhou, 2022, 10.1029/2021JB022964). It was observed that fracture length increases nonlinearly with $\sqrt{\tau}$ and then transitions to scaling law $\mathcal{L} = f(\mathcal{T})\sqrt{\tau}$, indicating that late-time fracture length increases linearly with the square root of cooling time. The scaling coefficient $f(\mathcal{T})$ shows the effects of inter-fracture stress interaction and *fracture arrest*. The solutions and scaling law provide fast predictions for all reservoir and cooling conditions using (single) model parameter $\mathcal{T}$. Application to the Utah FORGE EGS site with $\mathcal{T} = 0.11$ demonstrates that thermal fractures reach 0.67, 6.25, and 78.00 m in length, 0.49, 2.30, and 13.00 m in spacing, and 0.43, 2.09, and 12.19 mm in surface aperture at 1, 100 and 10,000 days. Second, numerical modeling of thermal fractures from two parallel hydraulic fractures was conducted and the modeling results show that it is effective for thermal fractures from different hydraulic fractures to eventually merge and connect, thus enhancing fracture connectivity and permeability. For a cooling of 150 °C at the Utah FORGE site, thermal fractures will connect two neighboring hydraulic fractures with 20 m spacing in ~150 days of EGS operation.

1. INTRODUCTION

In the current concept of an enhanced geothermal system (EGS), a pair of horizontal wells is drilled and stimulated, resulting in parallel hydraulic fractures that connect the two wells. Cold water is injected through the injection well, while hot water is produced in the production well for power generation. A cooled zone in the hydraulic fractures will propagate with time from the injection well to the production well, eventually leading to thermal breakthrough and power generation shutdown. Under natural conditions, the stimulated hydraulic fractures have different aperture and spacing that vary spatially and water circulation may result in much earlier breakthrough, affecting reservoir sustainability and shortening the lifespan of power generation.

Cooling of hydraulic fractures by circulating water may produce secondary thermal fractures transverse to hydraulic fractures. The concept of secondary thermal fractures was proposed in the EGS with single penny-shaped hydraulic fracture in the 1970s (Barr, 1980; Demuth & Harlow, 1980; Harlow & Pracht, 1972; Murphy, 1978) and extended to interpret field observations of thermal fracturing in water-flooding fields (Perkins and Gonzalez, 1985). The key features of these thermal fractures include (1) enhancement of heat-transfer area between fractures and the rock matrix, and (2) enhancement of fracture permeability through the improved connectivity between hydraulic and thermal fractures. Both types of enhancement can help reservoir sustainability during EGS operations, but have attracted little attention in EGS operation.

In this study, one of our objectives is to theoretically address different types of thermal fracturing in subsurface applications (Chen and Zhou, 2022). We (1) combine the advanced modeling theories and approaches for thermal shock fracturing (e.g., the stability analysis) and hydraulic fracturing (e.g., scaling analysis and the displacement discontinuity method, DDM), (2) obtain dimensionless solutions and late-time generic scaling behavior of fracture length, spacing, and aperture, (3) better understand the underlying mechanisms (i.e., inter-fracture stress interaction and fracture arrest) by comparing solutions of single fractures, constantly spaced multiple fractures (without arrest), and dynamically spaced multiple fractures (with arrest), and (4) systematically investigate the propagation and arrest of thermal fractures in deep formations under injection/flow conditions. For the scenario of thermal fracturing with negligible heat convection shown in Figure 1, the obtained dimensionless solutions are profiles for fracture spacing, length, and aperture, as a function of one dimensionless model parameter that cover the entire spectrum of rock properties, in situ confining stress, fluid pressure, and cooling conditions. In

contrast, numerous simulations using traditional numerical simulators are needed for different combinations of the properties and conditions.

We focus on the first scenario with one-dimensional heat conduction and negligible heat convection using a plane strain model (see Figure 1a in Chen and Zhou, 2022). The paper is organized as follows. First, the governing equations for heat conduction and thermoelastic deformation and the criteria for fracture propagation and arrest are given and converted to their dimensionless counterparts using scaling analysis in section 2. Second, the dimensionless solutions and scaling laws of single thermal fracture (Case A), constantly spaced multiple fractures (Case B), and dynamically spaced multiple fractures (Case C) are presented in section 3. These solutions are compared to show the effects of inter-fracture stress interaction and fracture arrest. Third, the verification of the dimensionless solutions using a FEM-based fracture model and the application of the Case C solution to a real-world geothermal reservoir to predict the evolution and pattern of thermal fractures are given in section 4. Finally, we present the results of numerical modeling of thermal fracturing between two parallel hydraulic fractures and show the effectiveness of thermal fractures in forming a well-connected hydraulic-thermal fracture network.

2. PROBLEM FORMULATION, GOVERNING EQUATIONS AND NON-DIMENSIONALIZATION

The fracturing driven by thermal stresses, in the absence or presence of pressure increase, of interest in this study is referred to hereafter as *thermal fracturing*, and the thermally driven fractures are referred to as *thermal fractures*. When initiated, they are densely spaced at the cooling wall or surface. Some of the initiated fractures continue to propagate with time, while the others are arrested at different times and distances from the cooling surface under strong inter-fracture stress interaction. The fracture propagation and arrest lead to fracture spacing that changes with time and distance (referred to as *dynamic spacing*) and a hierarchical pattern of propagating and arrested fractures (referred to as *dynamically spaced fractures*), which is very different from that of hydraulic fracturing (Chen and Zhou, 2021, 2022).

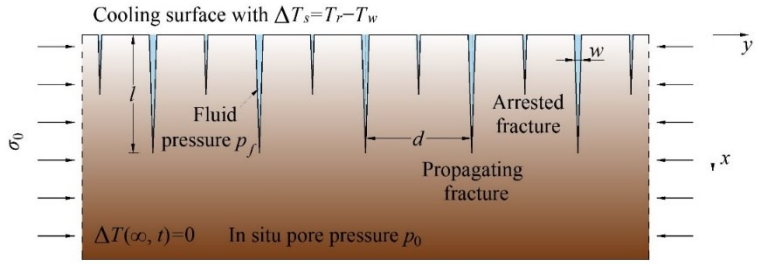

Figure 1: Schematic of propagation and arrest of thermal fractures of length l, spacing d, and aperture profile w, initiated at the surface with a cooling of ΔT_s and fluid pressure of p_f in a half-plane, under in situ confining stress of σ_0 and pore pressure of p_0 (modified from Chen & Zhou (2022)).

The governing equations including (1) the elasticity equation with thermal stress, effective confining stress, and aperture-induced stress interaction between thermal fractures, (2) the criterion of fracture propagation, and (3) the criterion of fracture arrest (i.e., stability analysis) are listed in Figure 2. Also shown in Figure 2 are the scaling analysis and non-dimensionalization of fracture length l, fracture spacing d, and fracture aperture $w(x)$ and their counterparts $\mathcal{L}$, $\mathcal{D}$, and $\Omega(\mathcal{X})$. The only dimensionless model parameter is the dimensionless effective confining stress, $\mathcal{T}$, which is the ratio of the effective confining stress $\sigma_{ec}(=\sigma_0 - p_0)$ to the thermal stress at the cooling surface, with in situ confining stress σ_0 and fluid pressure p_0, where p_0 can be in situ pore fluid pressure or fracture fluid pressure.

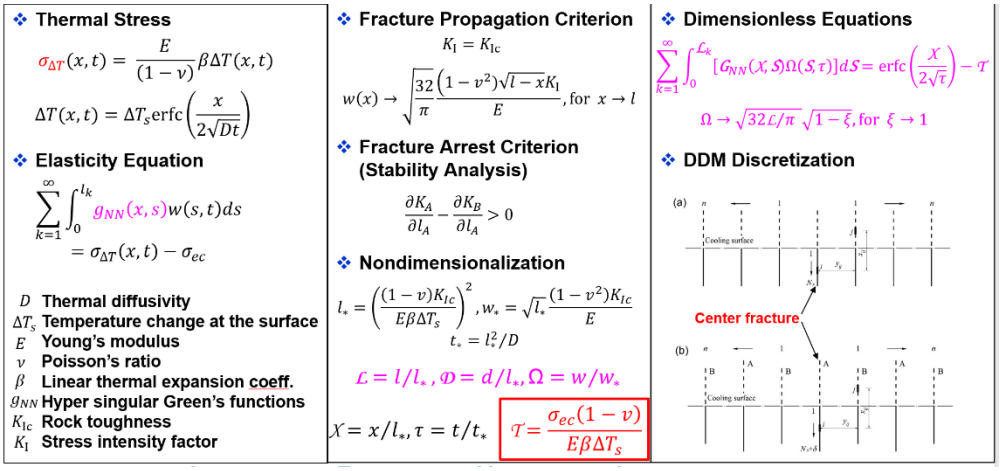

Figure 2: List of governing equations for elasticity, fracture propagation and arrest and their dimensionless counterparts after scaling analysis and non-dimensionalization.

3. DIMENSIONLESS SOLUTIONS AND SCALING LAWS

3.1 Single Thermal Fracture

Figure 3a shows that the dimensionless solutions of fracture length as a function of dimensionless time are profiles affected by dimensionless effective confining stress, the only dimensionless model parameter. For late-time fracture propagation, these profiles become straight lines in the double-log plot, indicating that a scaling law

$$\mathcal{L} = f(\mathcal{T})\sqrt{\tau}$$

can be used for fast prediction of dimensionless fracture length in terms of square root of dimensionless time τ. The scaling coefficient $f(\mathcal{T})$ shown in Figure 3b was derived analytically, with two asymptotic solutions for $\mathcal{T}\to 0$ or 1.

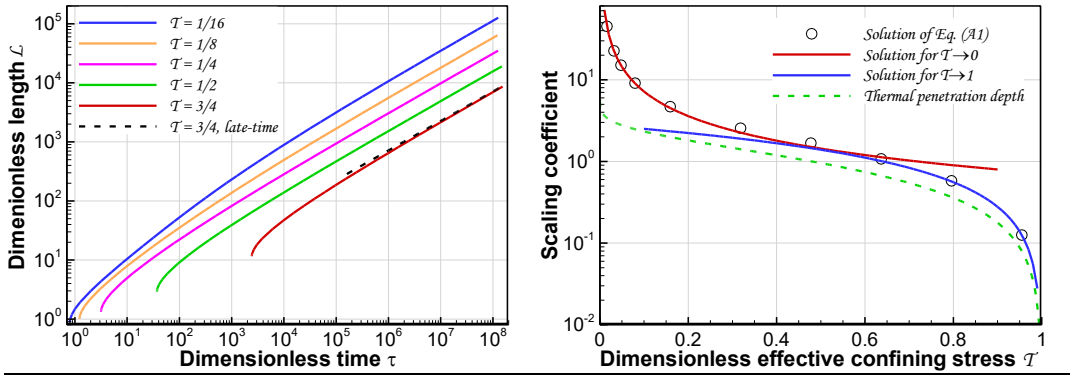

Figure 3: (Left) dimensionless fracture length $\mathcal{L}$ vs dimensionless time τ, as a function of dimensionless effective confining stress $\mathcal{T}$ (the only parameter), and (right) the scaling coefficient as a function of $\mathcal{T}$.

3.2 Dynamically Spaced Multiple Thermal Fractures

Figure 4 shows the solutions of dimensionless fracture length, spacing, and surface aperture at the cooling surface, as well as the effect of dimensionless effective confining stress $\mathcal{T}$ on these solutions.

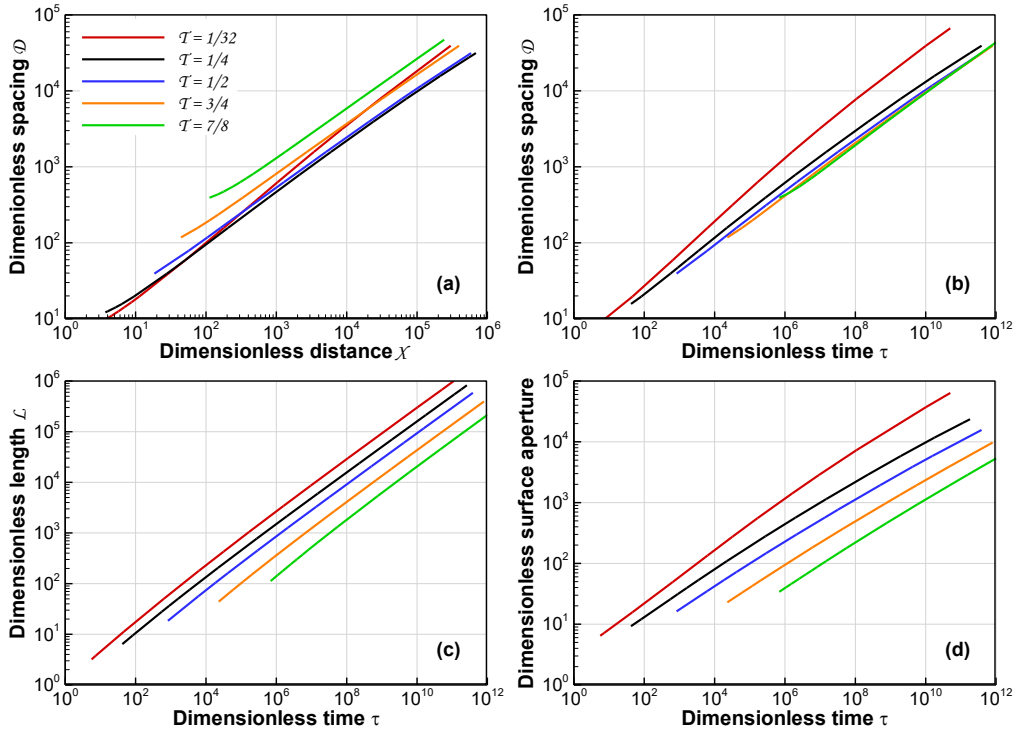

Figure 4: Evolution of dimensionless fracture spacing $\mathcal{D}$, length $\mathcal{L}$, and surface aperture Ω_0 under different dimensionless effective confining stress $\mathcal{T}$: (a) $\mathcal{D}(\mathcal{X})$, (b) $\mathcal{D}(\tau)$, (c) $\mathcal{L}(\tau)$, and (d) $\Omega_0(\tau)$

The late-time solutions also asymptotically approach to straight lines in the double-log plots. For dimensionless fracture length, we have the scaling law: $\mathcal{L} = f'(\mathcal{T})\sqrt{\tau}$, with scaling coefficient $f'(\mathcal{T}) < f(\mathcal{T})$, showing the effect of inter-fracture stress interaction and fracture arrest. These analytical solutions can be directly used for predicting the properties (length, spacing, aperture, and pattern) of thermal fractures for a real geothermal site, whose rock properties, stress and pressure condition, as well as cooling conditions can be grouped into one dimensionless parameter $\mathcal{T}$, as shown in section 4.

4. SOLUTION VALIDATION AND APPLICATIONS

The analytical solution of single fracture and the dimensionless solutions of dynamically spaced multiple fractures presented in section 3 (referred to hereafter as theoretical solutions) are first validated using a FEM-based fracture model. The solution of dynamically spaced fractures is then applied to several cases with elevated fluid pressure. For the validation and application, the rock properties and in situ conditions of pressure, temperature, and stresses from the Utah FORGE EGS site are used (see Table 1 in Chen and Zhou, 2022). The excellent agreement between the theoretical and FEM-based solutions for single thermal fracture is not shown here, but can be referred to Chen and Zhou (Figure 8, 2022). Figure 5 shows excellent agreement between theoretical solution (central line) and the FEM-based solution of fracture spacing, as well as two solutions of fracture length and surface aperture for the propagating period of four selected fractures in the FEM modeling.

The above validation for dynamically spaced fractures can be summarized: (1) the central-line theoretical solution can accurately predict the evolution of dynamic fracture spacing, (2) the arrest-line solutions can accurately predict the evolution of fracture length and surface aperture (as well as aperture profile along thermal fractures) for propagating fractures, and (3) the fully transient solution can predict the time-dependent pattern of propagating and arrested thermal fractures. When fracture pattern is not of interest, the profiles of central-line spacing and arrest-line length and surface aperture (prepared for different values of dimensionless effective confining stress) can be used directly for fast prediction.

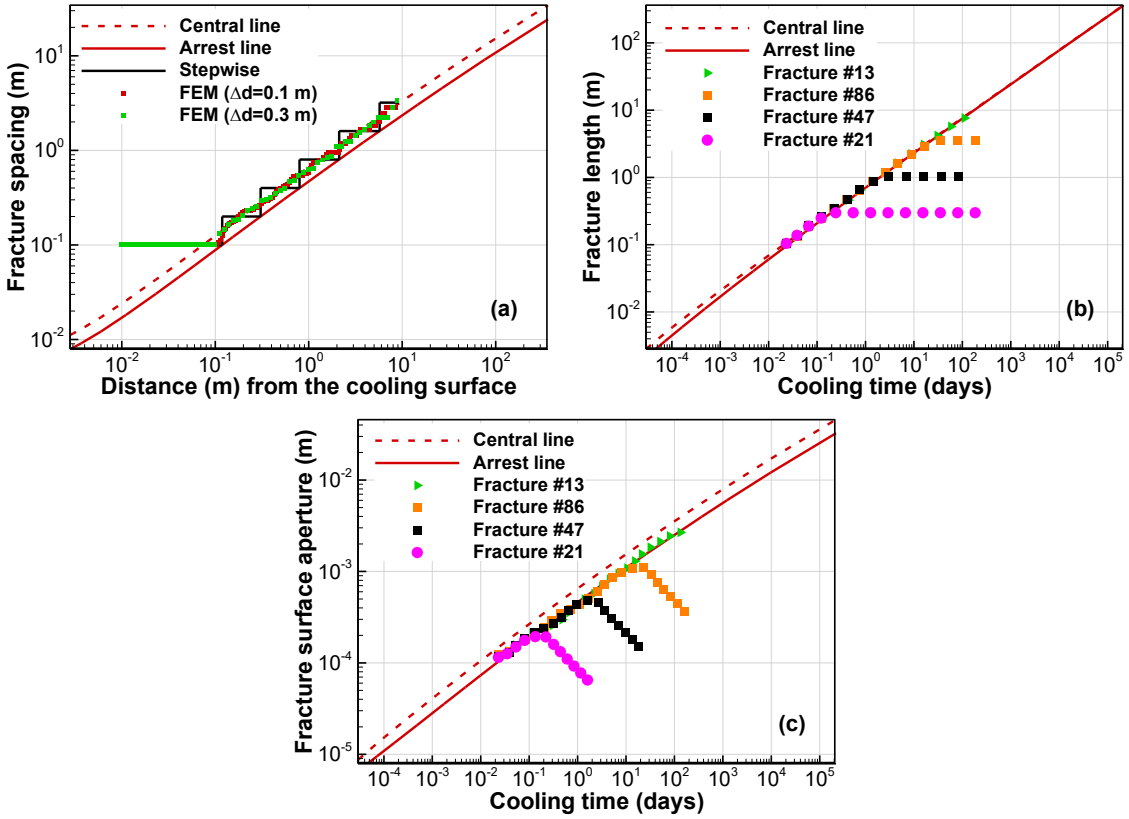

Figure 5: (a) Comparison between the uniform fracture spacing by the theoretical solution (stepwise, arrest and central lines) and the average spacing by the FEM solution, and comparison of (b) fracture length and (c) surface aperture between the theoretical solutions of propagating fractures and the FEM solutions of four selected fractures

Figure 6 shows excellent agreement between theoretical and FEM-based fracture pattern over 150 days of cooling and fracture propagation. The fracture patterns at any cooling time can also be seen from the figure. Note that the theoretical solutions were developed based on mode-I fracture propagation. However, these patterns are also in excellent agreement with the FEM-based patterns of mixed-mode fractures (see Figure 12 in Chen and Zhou, 2022).

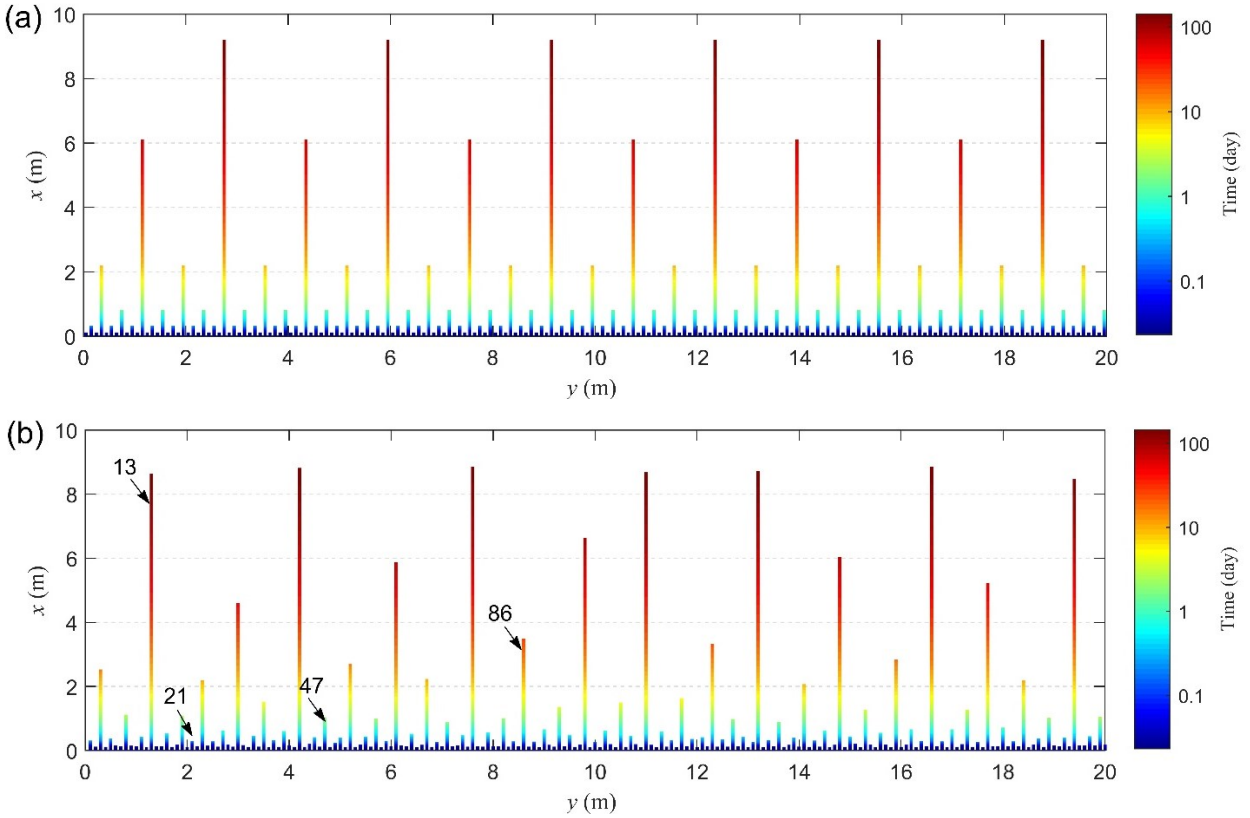

Figure 6: Comparison of propagation of thermal fractures for 150 days between (a) the fully transient theoretical solution and (b) the FEM solution. Each fracture is colored by cooling time (days) to show the dynamic evolution of fracture length and the arrest time can be seen at the tip of arrested fractures. The features of four selected individual fractures (#13, #21, #47, and #86) are shown in Figure 5

In addition to the base case, two additional fluid pressures (27.0 and 32.2 MPa) are used to investigate thermal fracturing under elevated pressure induced by water circulation. The effective confining stresses are $\sigma_{ec} = 5.2$ and 0 MPa, respectively. The fracture length in both cases is obtained using our theoretical arrest-line solution with $\mathcal{T} = 0.0583, 0.0$ and compared with the base-case solution (Figure 7). Fractures propagate in a similar way under the same thermal stress in all the cases. Note that the fluid pressure in thermal fractures only affect the dimensionless effective confining stress, $\mathcal{T}$; thermal fracturing is still controlled by thermal stress. When $\mathcal{T}<0$, hydraulic fracturing is dominant; thermal stress contributes to fracturing, but does not dominate fracturing.

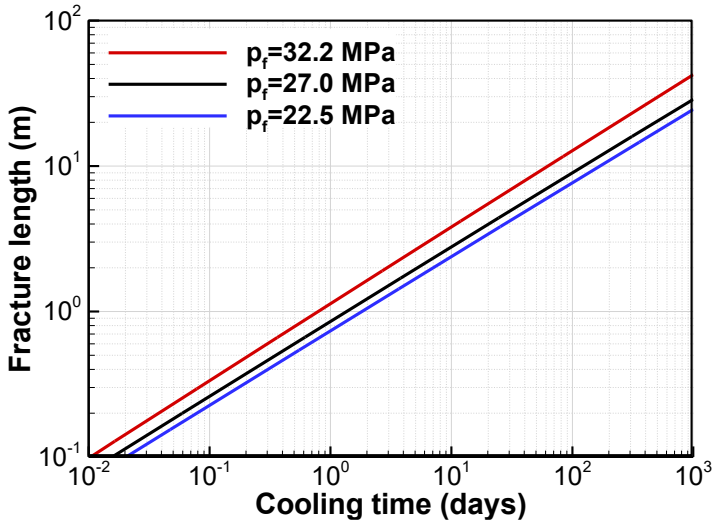

Figure 7: Evolution of fracture length under different fluid pressure in thermal fractures

5. NUMERICAL MODELING OF THERMAL FRACTURES BETWEEN TWO PARALLEL HYDRAULIC FRACTURES

Numerical modeling of thermal fracture propagation, arrest, and coalescence between two parallel hydraulic fractures was conducted for different hydraulic fracture spacing (Chen et al., 2023). The same rock properties and field conditions at the Utah FORGE EGS site were used. Figure 8 shows the fracture patterns at three different time for each case of hydraulic fracture spacing. Clearly, the coalescence of thermal fractures can be achieved within a short time for 20 m spaced hydraulic fractures in comparison with several decades of EGS operation. For an EGS with multi-stage hydraulic stimulation, the spacing of hydraulic fractures is expected to be smaller than 20 m for those stimulated in the same stimulation stage; for those hydraulic fractures between different stages, their spacing may not be far larger than 20 m. As a result, thermal fracturing will play a significant role in forming a well-connected network of hydraulic and thermal fractures. This effect of secondary, transverse thermal fractures that has not been studied before needs to be considered in EGS operation.,

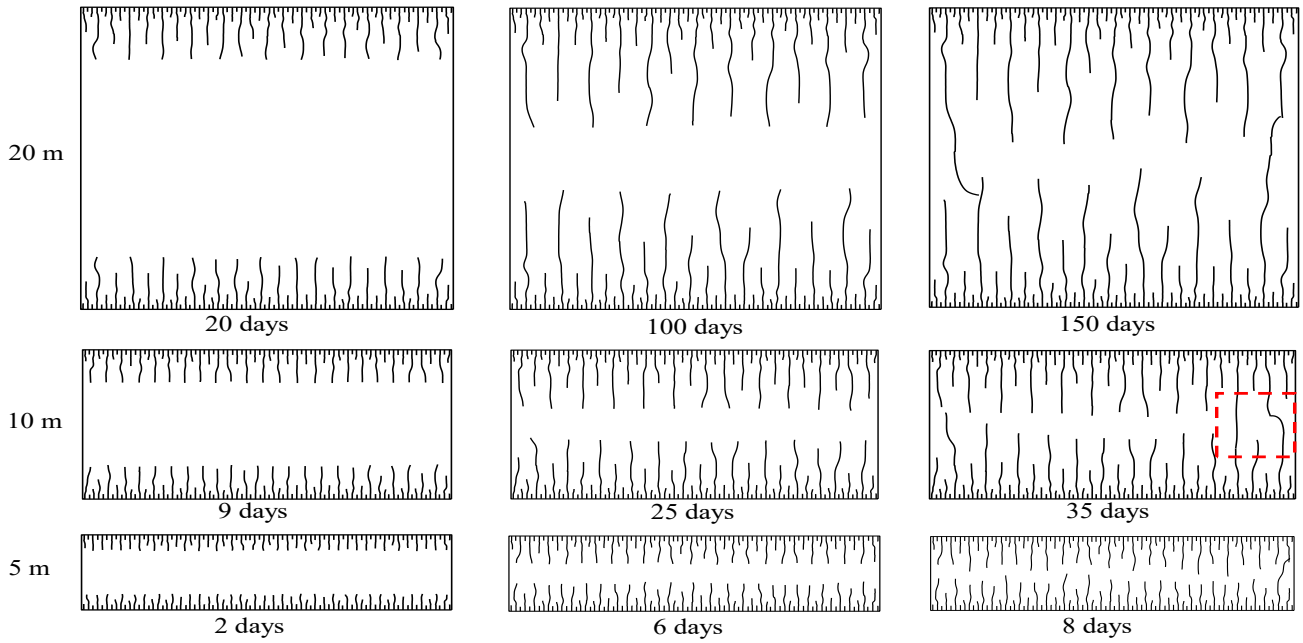

Figure 8: Pattern of propagating and arrested thermal fractures between two hydraulic fractures, as well as their coalescence.

6. CONCLUSIONS

In the current concept of multi-stage stimulation of an enhanced geothermal system, multiple hydraulic fractures stimulated will connect the injection and production wells, and cold water will be injected and circulated between the pair of wells. Significant cooling will occur in the hydraulic fractures and induce strong thermal stress. The thermal stress may induce secondary thermal fractures transverse to these hydraulic fractures. Eventually the thermal fractures will connect the hydraulic fractures and form a well-connected network of hydraulic and thermal fractures. The effect of thermal fracturing on EGS operation and reservoir sustainability has not be studied.

First, we developed analytical solutions of length, spacing, aperture, and pattern of evolving thermal fractures. Stability analysis was introduced for fracture arrest, dimensionless governing equations with one parameter were derived, DDM was used to discretize all thermal fractures, and two special algorithms were developed for analytical modeling of dynamically spaced fractures. Transient dimensionless solutions of length, spacing, and aperture (and pattern) of multiple thermal fractures were obtained and validated. Scaling laws of late-time fracture length (linear with square root of cooling time) were obtained for single and multiple thermal fractures. The solutions and scaling laws provide time profiles as a function of thermal stress ratio (dimensionless effective confining stress) that covers all reservoir and cooling conditions. These solutions and scaling laws can be easily applied to any geothermal site by using one single model parameter.

Second, coalescence of thermal fractures propagating from two neighboring parallel hydraulic fractures was simulated numerically. Results show how a well-connected network of hydraulic and thermal fractures is developed to enhance fracture-matrix heat transfer. The time scale for such a network to develop is relatively short in comparison with EGS operation lifespan. For a 20 m spacing of hydraulic fractures, the time scale for the Utah FORGE EGS site is on the order of 150 days, indicating that thermal fracturing is ***effective***. The effect of thermal fracturing on the evolution of fracture network and reservoir sustainability is needed to considered in EGS operation.

REFERENCES

Barr, D. T. (1980). Thermal cracking in nonporous geothermal reservoirs. (Master thesis), Massachusetts Institute of Technology.

Chen, B., & Zhou, Q. L. (2021). Propagation, arrest, and reactivation of thermally driven fractures in an unconfined half-space using stability analysis. Theoretical and Applied Fracture Mechanics, 102969. https://doi.org/10.1016/j.tafmec.2021.102969

Chen, B., & Zhou, Q. (2022). Scaling behavior of thermally driven fractures in deep low-permeability reservoirs: a plane strain model with 1-D heat conduction. *Journal of Geophysical Research - Solid Earth*, 127, e2021JB022964. https://doi.org/10.1029/2021JB022964.

Chen, B., Zhou, Q., & Wang, Y. (2023). Coalescence of thermal fractures initiated at parallel cooling surfaces, *Engineering Computations* (submitted).

Demuth, R. B., & Harlow, F. H. (1980). Geothermal energy enhancement by thermal fracture. Los Alamos Scientific Lab, NM (USA). https://doi.org/10.2172/6731510

EGI. (2019). Frontier observatory for research in geothermal energy – Milford site, Utah, phase 2c section b: results ii. Dynamic reservoir modeling. Energy and Geoscience Institute, University of Utah.

Harlow, F. H., & Pracht, W. E. (1972). A theoretical study of geothermal energy extraction. *Journal of Geophysical Research* (1896-1977), 77(35), 7038-7048. https://doi.org/10.1029/JB077i035p07038

Murphy, H. D. (1978). Thermal stress cracking and the enhancement of heat extraction from fractured geothermal reservoirs. Los Alamos Scientific Lab., N. Mex. (USA). https://doi.org/10.2172/6771724